Generalized diffusion model in optical tomography with clear layers

Guillaume Bal and Kui Ren

Department of Applied Physics and Applied Mathematics, Columbia University, New York New York 10027

Received February 17, 2003; revised manuscript received July 15, 2003; accepted August 20, 2003

We introduce a generalized diffusion equation that models the propagation of photons in highly scattering domains with thin nonscattering clear layers. Classical diffusion models break down in the presence of clear layers. The model that we propose accurately accounts for the clear-layer effects and has a computational cost comparable to that of classical diffusion. It is based on modeling the propagation in the clear layer as a local tangential diffusion process. It can be justified mathematically in the limit of small mean free paths and is shown numerically to be very accurate in two- and three-dimensional idealized cases. We believe that this model can be used as an accurate forward model in optical tomography. © 2003 Optical Society of America

OCIS codes: 170.0170, 170.3010, 170.3660, 170.3880, 170.6960, 170.7050.

1. INTRODUCTION

Optical tomography is increasingly being used as a medical imaging tool to assess the scattering and absorbing properties of human tissues probed by near-infrared photons. Several studies[1–8] have been done on the practical, theoretical, and computational aspects of optical tomography. Among other applications, optical tomography is being regarded as an interesting technique to image tumors and to monitor cerebral oxygenation in neonates. The latter is the application of interest in this paper.

Photon propagation in human tissues is best modeled by a radiative transport equation that describes the density of photons in the phase space, i.e., as a function of position and direction. Although such models are quite expensive computationally, they are being used increasingly often.[9] For computational savings an approximation to radiative transport is often preferred. It takes the form of a diffusion equation, which models photon density only spatially. The regime of validity of diffusion has been studied extensively.[1,10,11] Essentially, the diffusion equation can be used when tissue scattering is high and absorption small, which is the case for almost all human tissues in the head, the exception being a thin layer filled with cerebrospinal fluid. This layer is almost collisionless and absorptionless. Diffusion models perform very poorly in such layers.[12–15] Thus, diffusion models have to be modified for imaging oxygenation in the head of neonates.

One could certainly solve phase-space transport equations instead of the inaccurate diffusion equations.[12,16] A large literature exists on numerical techniques that allow us to use coarser schemes (modeling transport or diffusion equations) in the regions where multiple scattering makes the simulation relatively straightforward and finer schemes in the vicinity of the clear layer where transport effects must be calculated accurately.[17–21]

Because clear layers are by nature thin, an alternative solution exists to solving transport equations. A lot of work has been done by Arridge and his collaborators to develop hybrid models that would solve a diffusion equation in cases where the tissues are highly scattering and would model the transport behavior in a clear layer.[13–15] Similar models have been developed by one of the authors with an approach based on the asymptotic expansion of transport equations.[22,23] The models that came out of this research have the following common features. (1) They are diffusion equations with matching conditions at the boundary of the layer that account for the guiding effect of the clear layer. (2) These matching conditions take the form of nonlocal interface conditions for the photon density and current. (3) These models are quite accurate in practice, for solving both forward and inverse problems. (4) Their computational cost is much lower than that of full transport equations. (5) However, the cost is often significantly higher than the cost of the classical diffusion models and the models are quite complicated to implement.

In this paper we build on the asymptotic expansion techniques[22,23] to propose a new model that accurately models the clear-layer effects for a computational cost and an implementation by the finite-element method that are essentially the same as those of the classical diffusion model. The model is obtained by localizing the interface conditions at the clear layer. This local interface condition models a tangential diffusion process that accounts for the propagation of photons along the clear layer. In variational form, this diffusion process is about as easy to solve as the classical volume diffusion process.

The rest of the paper is structured as follows. Section 2 recalls some results on the transport and classical diffusion models. Section 3 presents the new generalized diffusion model with local interface conditions. Explicit expressions are obtained for the tangential diffusion equation in the case of two-dimensional circular clear layers. Section 4 confirms numerically the accuracy of the model in the idealized cases of circular clear layers within the unit disk in a two-dimensional setting and spherical clear layers within the unit sphere in a three-dimensional setting. Section 5 offers some conclusions.

1084-7529/2003/122355-10$15.00

2. TRANSPORT AND DIFFUSION MODELS

We model photon propagation in human tissues by the following steady-state linear radiative transfer equation:

$$\mathbf{\Omega}\cdot\nabla u(\mathbf{x},\,\mathbf{\Omega})+\sigma_a(\mathbf{x})u(\mathbf{x},\,\mathbf{\Omega})+Q(u)(\mathbf{x},\,\mathbf{\Omega})=S(\mathbf{x}),\quad \text{in}\quad \mathcal{D}\times S^{n-1},$$

$$u(\mathbf{x},\,\mathbf{\Omega})=g(\mathbf{x},\,\mathbf{\Omega})\quad \text{on}\quad \Gamma_-=\{(\mathbf{x},\,\mathbf{\Omega})\in\partial\mathcal{D}\times S^{n-1}\ \text{s.t.}\ \mathbf{\Omega}\cdot\boldsymbol{\nu}(\mathbf{x})<0\}. \quad (1)$$

Here $u(\mathbf{x},\,\mathbf{\Omega})$ is the photon flux intensity at point $\mathbf{x}\in\mathcal{D}$, where $\mathcal{D}$ is a subset in $\mathbb{R}^n$, with direction of propagation $\mathbf{\Omega}\in S^{n-1}$, where S^{n-1} is the unit sphere in $\mathbb{R}^n$. The space dimension is $n=3$ in practice. In this paper we consider $n=2$, because it is computationally simpler, and $n=3$. The source of photons at the boundary of the domain is given by $g(\mathbf{x},\,\mathbf{\Omega})$, and the outward unit normal to the domain is $\boldsymbol{\nu}(\mathbf{x})$ at $\mathbf{x}\in\partial\mathcal{D}$. The volume source of the photons is given by $S(\mathbf{x})$. The absorption coefficient is denoted by $\sigma_a(\mathbf{x})$, and the scattering operator Q is defined as

$$Q(u)(\mathbf{x},\,\mathbf{\Omega})=\sigma_s(\mathbf{x})\left[u(\mathbf{x},\,\mathbf{\Omega})-\int_{S^{n-1}}u(\mathbf{x},\,\mathbf{\Omega}')\mathrm{d}\mu(\mathbf{\Omega}')\right]. \quad (2)$$

Here $\sigma_s(\mathbf{x})$ is the scattering coefficient and $\mathrm{d}\mu$ is the surface measure on S^{n-1} normalized so that $\int_{S^{n-1}}\mathrm{d}\mu(\mathbf{\Omega})=1$.

In two space dimensions, we parameterize $\mathbf{\Omega}=(\cos\theta,\sin\theta)$ and have

$$\int_{S^1}u(\mathbf{x},\,\mathbf{\Omega})\mathrm{d}\mu(\mathbf{\Omega})=\frac{1}{2\pi}\int_0^{2\pi}u(\mathbf{x},\,\theta)\mathrm{d}\theta,$$

identifying $u(\mathbf{x},\,\mathbf{\Omega})$ with $u(\mathbf{x},\,\theta)$. In three space dimensions, we parameterize $\mathbf{\Omega}=(\sin\theta\cos\phi,\sin\theta\sin\phi,\cos\theta)$ and have

$$\int_{S^2}u(\mathbf{x},\,\mathbf{\Omega})\mathrm{d}\mu(\mathbf{\Omega})=\frac{1}{4\pi}\int_0^{2\pi}\int_0^{\pi}u(\mathbf{x},\,\theta,\,\phi)\sin\theta\mathrm{d}\theta\mathrm{d}\phi,$$

identifying $u(\mathbf{x},\,\mathbf{\Omega})$ with $u(\mathbf{x},\,\theta,\,\phi)$.

The optical tomography problem consists of reconstructing $\sigma_a(\mathbf{x})$ and $\sigma_s(\mathbf{x})$ from boundary measurements $u(\mathbf{x},\,\mathbf{\Omega})$ for $\mathbf{x}\in\partial\mathcal{D}$ and $\mathbf{\Omega}\in S^{n-1}$. This is quite a difficult problem both in theory and in practice.[1,3,6,9,24,25] This problem is also very expensive computationally because the radiative transfer equations are posed in the phase space, with a minimum of three spatial variables and two angular variables in practical calculations. They are therefore often replaced by their diffusion approximations, which do not involve any angular variable.

Diffusion approximations are valid in the regime of high scattering $\sigma_s\gg 1$ and small absorption $\sigma_a\ll 1$. We can then approximate the solution $u(\mathbf{x},\,\mathbf{\Omega})$ by

$$u(\mathbf{x},\,\mathbf{\Omega})=U(\mathbf{x})-\frac{1}{\sigma_s(\mathbf{x})}\mathbf{\Omega}\cdot\nabla U(\mathbf{x})+\text{smaller-order terms}, \quad (3)$$

where $U(\mathbf{x})$ is the solution to the following diffusion equation,

$$-\nabla\cdot D(\mathbf{x})\nabla U(\mathbf{x})+\sigma_a(\mathbf{x})U(\mathbf{x})=S(\mathbf{x})\quad \text{in}\quad \mathcal{D},$$

$$U(x)+nL_nD(\mathbf{x})\boldsymbol{\nu}(\mathbf{x})\cdot\nabla U(x)=g(\mathbf{x})\quad \text{on}\quad \partial\mathcal{D}, \quad (4)$$

where we assume that $g(\mathbf{x},\,\mathbf{\Omega})=g(\mathbf{x})$ does not depend on $\mathbf{\Omega}$ to simplify and where the diffusion coefficient is defined by

$$D(\mathbf{x})=\frac{1}{n\sigma_s(\mathbf{x})},\qquad n=2,3. \quad (5)$$

The extrapolation length L_n accounts for the leakage of photons at the domain boundary. Approximate values are $L_2=0.8164$ and $L_3=0.7104$ for isotropic scattering.[10,22,26,27] Diffusion equations are very well studied both mathematically and physically and can be justified by various means.[1,10,11]

The diffusive regime is valid in most human tissues, where absorption is relatively small and scattering quite large, with typical values of the order of $\sigma_a=0.1\,\mathrm{cm}^{-1}$ and $\sigma_s=20\,\mathrm{cm}^{-1}$. This corresponds to an absorption mean free path of 10 cm and a scattering mean free path of 0.05 cm. Notice that $D(\mathbf{x})$ and $\sigma_a(\mathbf{x})$ in Eqs. (4) are then of comparable order.

The presence of cerebrospinal fluid in the human head prevents the use of classical diffusion equations (4). The reason is that this fluid is optically clear: Photons propagate along straight lines almost scattering-free in such fluids. This creates a guiding effect that diffusion equation (4) cannot capture. Several studies have been conducted to understand and fix this problem.[13,14,22,23,28] The main idea consists of using the diffusion equation where it is valid and coupling it with a local transport equation in the nonscattering regions. An asymptotic analysis[23] justifies such an approach for thin clear inclusions. Several such hybrid models have been analyzed numerically.[22] This analysis shows the adequacy and robustness of the models. The main difficulty is that the models' numerical implementation is still difficult and their cost significantly higher than that of the classical diffusion mode (4) although much lower than that of the full transport equation (1). It is the objective of this paper to further simplify the hybrid model and obtain a scheme that is both accurate and computationally efficient.

3. GENERALIZED DIFFUSION MODEL

Following an earlier asymptotic derivation,[23] we propose here what we believe is the simplest model that captures both the diffusive behavior outside the clear layer and the guiding effect within the clear layer. It is based on solving a diffusion equation with local jump conditions at the clear layer.

A. Notation and Geometry

The geometry of the clear layer $\mathcal{D}^C$ is as follows. We define Σ as a closed smooth surface embedded in $\mathcal{D}$ and

$$\mathcal{D}^C = \{\mathbf{y} \in \mathcal{D} \text{ s.t. } \mathbf{y} = \mathbf{x} + t\boldsymbol{\nu}(\mathbf{x}), \quad \text{with} \quad \mathbf{x} \in \Sigma \quad \text{and} \quad |t| < L\}. \tag{6}$$

Here L is a fixed sufficiently small number and $\boldsymbol{\nu}(\mathbf{x})$ is the outward normal to (the volume inside) Σ at $\mathbf{x} \in \Sigma$. We denote by Σ^E and Σ^I the outer and inner surfaces of $\mathcal{D}^C$ and assume that these surfaces are smooth; see Fig. 1. We define $\boldsymbol{\nu}_C(\mathbf{x})$ as the outward unit normal to $\mathcal{D}^C$ at a point $\mathbf{x} \in \partial\mathcal{D}^C = \Sigma^E \cup \Sigma^I$. For $\mathbf{x} \in \Sigma$, we define

$$\mathbf{x}^E = \mathbf{x} + L\boldsymbol{\nu}(\mathbf{x}) \in \Sigma^E, \qquad \mathbf{x}^I = \mathbf{x} - L\boldsymbol{\nu}(\mathbf{x}) \in \Sigma^I. \tag{7}$$

It is useful to see $\mathbf{x}^E$ and $\mathbf{x}^I$ as functions of $\mathbf{x} \in \Sigma$. Notice that the outward normal to $\mathcal{D}^C$ at $\mathbf{x}^E \in \Sigma^E$ is $\boldsymbol{\nu}_C(\mathbf{x}^E) = \boldsymbol{\nu}(\mathbf{x})$ and the outward normal at $\mathbf{x}^I \in \Sigma^I$ is $\boldsymbol{\nu}_C(\mathbf{x}^I) = -\boldsymbol{\nu}(\mathbf{x})$.

The solution operator to the radiative transfer equation in $\mathcal{D}^C$ is denoted by $\mathcal{R}^C$. Let us define

$$\Gamma^C_{\pm} = \{(\mathbf{x}, \boldsymbol{\Omega}) \in \partial\mathcal{D}^C \times S^{n-1} \text{ s.t. } \pm\boldsymbol{\Omega}\cdot\boldsymbol{\nu}_C(\mathbf{x}) > 0\},$$

and consider the problem inside the layer

$$\boldsymbol{\Omega}\cdot\nabla v(\mathbf{x}, \boldsymbol{\Omega}) + \sigma_a(\mathbf{x})v(\mathbf{x}, \boldsymbol{\Omega}) + Q(v)(\mathbf{x}, \boldsymbol{\Omega}) = 0, \quad \text{in} \quad \mathcal{D}^C \times S^{n-1},$$

$$v(\mathbf{x}, \boldsymbol{\Omega}) = g(\mathbf{x}, \boldsymbol{\Omega}) \qquad \text{on} \quad \Gamma^C_-.$$

We then define $\mathcal{R}^C$ as the operator that maps $g(\mathbf{x}, \boldsymbol{\Omega})$ on Γ^C_- to $v(\mathbf{x}, \boldsymbol{\Omega})|_{\Gamma^C_+} = \mathcal{R}^C g(\mathbf{x}, \boldsymbol{\Omega})$, the restriction to the transport solution $v(\mathbf{x}, \boldsymbol{\Omega})$ to the outgoing surface (in the phase space) Γ^C_+. Such an operator is well defined in suitably chosen weighted L^p spaces.[10]

We now define the operator $\mathcal{R}^C_1$ by

$$\mathcal{R}^C_1 = \mathcal{R}^C - \mathcal{I}, \tag{8}$$

where the near-identity operator $\mathcal{I}$ is defined from Γ^C_- to Γ^C_+ by

$$\mathcal{I}u(\mathbf{x}, \boldsymbol{\Omega}) = \begin{cases} u(\mathbf{x} + 2L\boldsymbol{\nu}(\mathbf{x}), \boldsymbol{\Omega}), & \mathbf{x} \in \Sigma^I \\ u(\mathbf{x} - 2L\boldsymbol{\nu}(\mathbf{x}), \boldsymbol{\Omega}), & \mathbf{x} \in \Sigma^E. \end{cases}$$

This near-identity operator $\mathcal{I}$ is merely a translation from the inner boundary to the outer boundary and vice versa. This is an approximation to what happens to most photons that cross the clear layer: Since the clear layer is optically thin (because σ_s is small in $\mathcal{D}^C$) and most photons reach the clear layer at $\mathbf{x}^I$ with an incidence angle far from orthogonal to $\boldsymbol{\nu}(\mathbf{x})$, the photons do not propagate for a long time in the clear layer, and they exit it at a point near $\mathbf{x}^E$. For those relatively rare photons that reach the clear layer with a direction almost orthogonal to $\boldsymbol{\nu}(\mathbf{x})$, the exit point will no longer be $\mathbf{x}^E$. This behavior is captured by $\mathcal{R}^C_1$ and modifies the local current equilibrium.

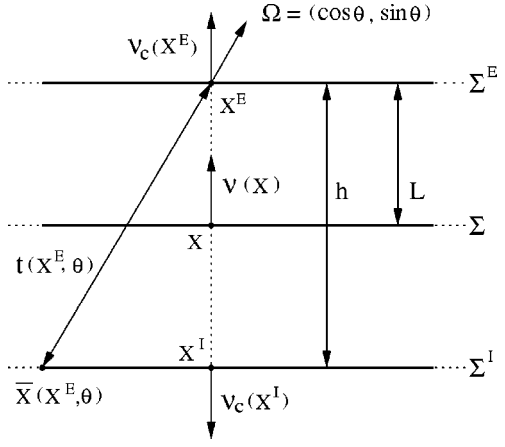

Fig. 1. Local geometry of the clear layer.

B. Generalized Diffusion Equation with Nonlocal Interface Conditions

It was shown (Ref. 23, p. 1687) that a good approximation of $u(\mathbf{x}, \boldsymbol{\Omega})$, the solution to Eq. (1), was given by $U(\mathbf{x})$ solution of

$$\begin{aligned} -\nabla\cdot D(\mathbf{x})\nabla U(\mathbf{x}) + \sigma_a(\mathbf{x})U(\mathbf{x}) &= S(\mathbf{x}) \qquad \text{in} \quad \mathcal{D}\backslash\mathcal{D}^C, \\ U(\mathbf{x}) + nL_n D(\mathbf{x})\boldsymbol{\nu}(\mathbf{x})\cdot\nabla U(\mathbf{x}) &= g(\mathbf{x}) \qquad \text{on} \quad \partial\mathcal{D}, \\ U(\mathbf{x}^E) &= U(\mathbf{x}^I) \qquad \text{on} \quad \Sigma, \\ \boldsymbol{\nu}(\mathbf{x})\cdot D(\mathbf{x}^E)\nabla U(\mathbf{x}^E) - \boldsymbol{\nu}(\mathbf{x})\cdot D(\mathbf{x}^I)\nabla U(\mathbf{x}^I) &= KU(\mathbf{x}) \qquad \text{on} \quad \Sigma, \end{aligned} \tag{9}$$

where the integral operator K is given by

$$KU(\mathbf{x}) = \int_{\Gamma_+(\mathbf{x}^E)} \boldsymbol{\Omega}\cdot\boldsymbol{\nu}_C(\mathbf{x}^E)(\mathcal{R}^C_1 U)(\mathbf{x}^E, \boldsymbol{\Omega})\mathrm{d}\mu(\boldsymbol{\Omega}) + \int_{\Gamma_+(\mathbf{x}^I)} \boldsymbol{\Omega}\cdot\boldsymbol{\nu}_C(\mathbf{x}^I)(\mathcal{R}^C_1 U)(\mathbf{x}^I, \boldsymbol{\Omega})\mathrm{d}\mu(\boldsymbol{\Omega}). \tag{10}$$

We have defined $\Gamma_+(\mathbf{x}) = \{\boldsymbol{\Omega} \in S^{n-1} \text{ s.t. } \boldsymbol{\Omega}\cdot\boldsymbol{\nu}_C(\mathbf{x}) > 0\}$ and have implicitly used that $\mathbf{x}^E$ and $\mathbf{x}^I$ defined in Eqs. (7) are functions of $\mathbf{x} \in \Sigma$. Notice that this diffusion problem is posed on $\mathcal{D}\backslash\mathcal{D}^C$. What happens inside the layer $\mathcal{D}^C$ is modeled by the operator $\mathcal{R}^C_1$ in the definition of K. The two jump conditions in Eqs. (9) indicate the boundary conditions satisfied by U at the boundary $\partial\mathcal{D}^C$. It has been shown[23] that the above problem [Eqs. (9)] was well-posed provided that the thickness of the layer L was sufficiently small. Numerical simulations based on Eqs. (9) and on similar generalized diffusion models[22,23] have shown the accuracy of the approximation.

The physical interpretation of the jump conditions is the following. The jump of the total flux vanishes, $U(\mathbf{x}^E) = U(\mathbf{x}^I)$, because the clear layer is not sufficiently thick to modify this equilibrium. However, it is sufficiently large to modify the current balance. The difference between currents crossing the interfaces of the clear layer is balanced by the current of photons inside the clear layer. The latter is modeled by $KU(\mathbf{x})$. As a minor remark, let us mention that the asymptotic expansion[23] involves an additional Jacobian term corresponding to the map $\mathcal{I}$. Since $\mathcal{I}$ is near identity, we have replaced the Jacobian by 1. Accounting for this Jacobian does not change the limiting equations that will be obtained below.

C. Localization of the Interface Conditions

We now aim at further simplifying Eqs. (9) by replacing the nonlocal operator K in Eq. (10) with its local approximation. In doing so, we will model the clear layer $\mathcal{D}^C$ by

a local jump condition for the diffusion solution at Σ. We assume that the clear layer is totally nonscattering, i.e., that $\sigma_s(\mathbf{x}) = 0$ for $\mathbf{x} \in \mathcal{D}^C$. This assumption is fairly accurate in practice. All the results that we present below are not significantly modified when the layer is weakly scattering; see our remarks at the end of the section.

Let us consider the two-dimensional case $n = 2$. Let $(\mathbf{x}, \boldsymbol{\Omega}) \in \Gamma_+^C$. We define $t(\mathbf{x}, \theta)$ as the time it takes to travel from Γ_-^C to $\mathbf{x}$ in the direction $-\boldsymbol{\Omega}$ (with unit speed). We also define $\bar{\mathbf{x}} = \bar{\mathbf{x}}(\mathbf{x}, \theta) = \mathbf{x} - t(\mathbf{x}, \theta)\boldsymbol{\Omega}$, the starting point on Γ_-^C. Since the clear layer is nonscattering, we obtain by solving the free transport equation along its characteristics that

$$\mathcal{R}^C U(\mathbf{x}, \theta) = \exp[-\sigma_a t(\mathbf{x}, \theta)] U(\bar{\mathbf{x}}),$$

assuming that absorption is constant in $\mathcal{D}^C$. Let us consider a point $\mathbf{x}^I \in \Sigma^I$ such that $\bar{\mathbf{x}}(\mathbf{x}^I, \theta) \in \Sigma^E$ for all θ such that $\boldsymbol{\nu}_C(\mathbf{x}^I) \cdot \boldsymbol{\Omega} > 0$. This means that the photons reaching $\mathbf{x}^I$ all come from the other interface Σ^E. We then have that the contribution to the current of photons crossing Σ^I is given by

$$\begin{aligned} J^I &= \int_{\Gamma_+(\mathbf{x}^I)} \boldsymbol{\Omega} \cdot \boldsymbol{\nu}_C(\mathbf{x}^I)(\mathcal{R}_1^C U)(\mathbf{x}^I, \boldsymbol{\Omega}) \mathrm{d}\mu(\boldsymbol{\Omega}) \\ &= \frac{1}{2\pi} \int_0^\pi \sin\theta \{\exp[-\sigma_a t(\mathbf{x}^I, \theta)] U(\bar{\mathbf{x}}^I) - U(\mathbf{x}^E)\} \mathrm{d}\theta, \end{aligned}$$

where θ is chosen so that $0 \leqslant \theta \leqslant \pi$ spans $\Gamma_-^C(\mathbf{x}^I)$. Notice that both $\bar{\mathbf{x}}^I$ and $\mathbf{x}^E$ belong to Σ^E. Locally around $\mathbf{x}^E$ we can parameterize Σ^E by the arc-length distance $s(\bar{\mathbf{x}}^I) \equiv s(\theta, \mathbf{x}^E)$ to $\mathbf{x}^E$. When the curvature of Σ is positive, all points $\bar{\mathbf{x}}^I$ are close to $\mathbf{x}^E$ since the clear layer is thin. We can thus use the Taylor expansion

$$\begin{aligned} U(\bar{\mathbf{x}}^I) &= U(\mathbf{x}^E) + s(\theta; \mathbf{x}^E) \frac{\partial U}{\partial s}(\mathbf{x}^E) \\ &\quad + \frac{1}{2} s^2(\theta; \mathbf{x}^E) \frac{\partial^2 U}{\partial s^2}(\mathbf{x}^E) + \text{smaller terms} \\ &= U(\mathbf{x}^E) + \frac{\partial}{\partial s}\left[\frac{s^2(\theta; \mathbf{x}^E)}{2} \frac{\partial U}{\partial s}\right](\mathbf{x}^E) \\ &\quad + \text{smaller terms}. \end{aligned} \tag{11}$$

Similarly, we have

$$\exp[-\sigma_a t(\mathbf{x}^I, \theta)] = 1 - \sigma_a t(\mathbf{x}^I, \theta) + \text{smaller terms}. \tag{12}$$

We finally obtain the following approximation,

$$\begin{aligned} J^I &= -\sigma_a^I(\mathbf{x}^I) U(\mathbf{x}^E) + b^I(\mathbf{x}^E) \frac{\partial U}{\partial s}(\mathbf{x}^E) + d^I(\mathbf{x}^E) \frac{\partial^2 U}{\partial s^2}(\mathbf{x}^E) \\ &\quad + \ldots \\ &= -\sigma_a^I(\mathbf{x}^I) U(\mathbf{x}^E) + \frac{\partial}{\partial s}\left[d^I(\mathbf{x}^E) \frac{\partial U}{\partial s}\right](\mathbf{x}^E) + \ldots, \end{aligned} \tag{13}$$

where

$$\begin{aligned} \sigma_a^I(\mathbf{x}^I) &= \sigma_a \frac{1}{2\pi} \int_0^\pi t(\mathbf{x}^I, \theta) \sin\theta \mathrm{d}\theta, \\ b^I(\mathbf{x}^E) &= \frac{1}{2\pi} \int_0^\pi s(\theta; \mathbf{x}^E) \sin\theta \mathrm{d}\theta, \\ d^I(\mathbf{x}^E) &= \frac{1}{2\pi} \int_0^\pi \frac{1}{2} s^2(\theta; \mathbf{x}^E) \sin\theta \mathrm{d}\theta. \end{aligned} \tag{14}$$

Notice that b^I vanishes when the surface Σ is symmetrical about $\mathbf{x}$ since then $s(\pi - \theta; \mathbf{x}^E) = -s(\theta; \mathbf{x}^E)$. This justifies that the asymptotic expansion is pushed to second order in Eq. (11). The local approximation to the contribution $KU(\mathbf{x}^E) - J^I$ can be obtained in a similar manner. Its calculation is slightly more complicated since it involves two contributions coming from photons that entered $\mathcal{D}^C$ through Σ^I and Σ^E.

Adding the contributions from the two layer boundaries and sending the thickness of the clear layer to zero (thus identifying $\mathbf{x}^E$ and $\mathbf{x}^I$ with $\mathbf{x} \in \Sigma$), we obtain that

$$\begin{aligned} KU(\mathbf{x}) &= \frac{\partial}{\partial s}\left[d^C(\mathbf{x}) \frac{\partial U}{\partial s}\right](\mathbf{x}) - \sigma_a^C(\mathbf{x}) U(\mathbf{x}) \\ &\quad + \text{smaller terms}. \end{aligned} \tag{15}$$

The diffusion coefficient d^C is positive, and the absorption coefficient σ_a^C is nonnegative. This implies that the asymptotic limit of the operator K is negative in the sense that neglecting smaller-order terms and integrating by parts, $\int_\Sigma (KU)(\mathbf{x}) U(\mathbf{x}) \mathrm{d}S(\mathbf{x}) \leqslant 0$ for smooth functions $U(\mathbf{x})$, where $\mathrm{d}S(\mathbf{x})$ is the surface measure on Σ.

The above procedure can be generalized to the three-dimensional case without any theoretical difficulty, although the local parameterization of the surfaces Σ^E and Σ^I and the calculation of the travel times $t(\mathbf{x}, \theta, \phi)$ and currents in Eq. (10) become more complicated.

D. Tangential Diffusion Coefficient for Circular Layers

In the rest of this paper we assume that the surface Σ is a circle of radius R in two space dimensions $n = 2$ and a sphere of radius R in three space dimensions $n = 3$; see Fig. 2. Also, to simplify, we assume that the clear layer is nonabsorbing, i.e., $\sigma_a(\mathbf{x}) = 0$ in $\mathcal{D}^C$. We then obtain that

$$KU(\mathbf{x}^E) = d^C \Delta_\perp U(\mathbf{x}^E) + \text{small terms}, \tag{16}$$

where $\Delta_\perp$ is the Laplace–Beltrami operator for the sphere when $n = 3$ (i.e., the Laplace operator in the tangent plane to the sphere) and $\Delta_\perp = \partial^2/\partial s^2$ for the circle when $n = 2$. The diffusion coefficient is given in two space dimensions by

$$\begin{aligned} d^C &= d^C_{\text{ex-ex}} + d^C_{\text{ex-in}} + d^C_{\text{in-ex}}, \\ d^C_{\text{ex-ex}} &= \frac{1}{2\pi} \int_0^{\theta_0} \sin\theta (R + L)^2 (2\theta)^2 \mathrm{d}\theta, \\ d^C_{\text{ex-in}} &= \frac{1}{2\pi} \int_{\theta_0}^{\pi/2} \sin\theta (R - L)^2 \\ &\quad \times \left[\theta - \arccos\left(\frac{R + L}{R - L} \cos\theta\right)\right]^2 \mathrm{d}\theta, \end{aligned}$$

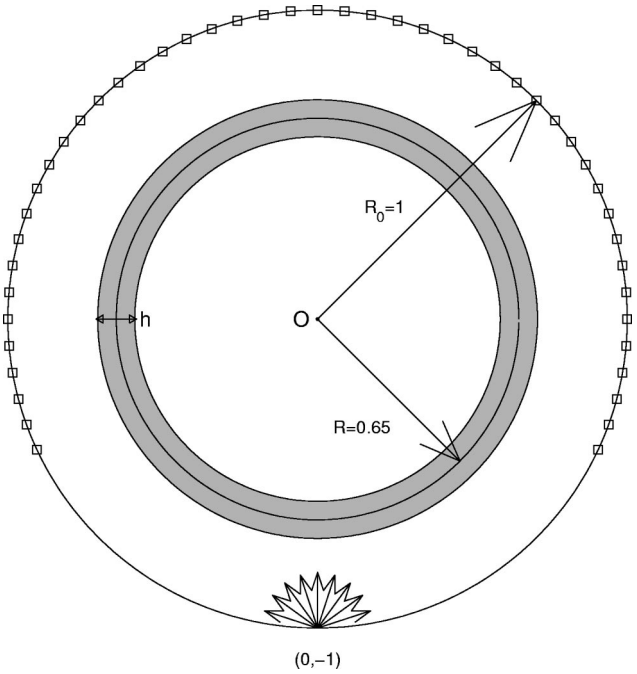

Fig. 2. Geometry of the two-dimensional setting and cross section of the geometry of the three-dimensional setting with azimuthal symmetry.

$$d^C_{\text{in-ex}} = \frac{1}{2\pi}\int_0^{\pi/2} \sin\theta(R+L)^2\left[-\theta + \arccos\left(\frac{R-L}{R+L}\cos\theta\right)\right]^2 \mathrm{d}\theta. \quad (17)$$

Here θ_0 is the limiting angle below which incident particles enter the clear layer through the upper surface and exit it through the same upper surface. It is defined by

$$\theta_0 = \arccos\left(\frac{R-L}{R+L}\right). \quad (18)$$

The three components of d^C are the contributions of photons that exit (enter) the clear layer through the upper (upper) surface ($d^C_{\text{ex-ex}}$), the upper (lower) surface ($d^C_{\text{ex-in}}$), and the lower (upper) surface ($d^C_{\text{in-ex}}$). Thus $d^C_{\text{in-ex}}$ is given by $d^I(\mathbf{x}^E)$ in Eqs. (14), and the other two contributions correspond to the photons crossing the clear layer through Σ^E.

A similar expression can be calculated for the tangential diffusion coefficient in three space dimensions. We have not reproduced this long expression here.

E. Generalized Diffusion Model with Local Interface Conditions

With the above approximations, the generalized diffusion model then takes the following form in the limit of vanishing thickness of the clear layer:

$$\begin{aligned}
-\nabla\cdot D(\mathbf{x})\nabla U(\mathbf{x}) + \sigma_a(\mathbf{x})U(\mathbf{x}) &= S(\mathbf{x}) && \text{in } \mathcal{D}\backslash\Sigma,\\
U(\mathbf{x}) + nL_n D(\mathbf{x})\boldsymbol{\nu}(\mathbf{x})\cdot\nabla U(\mathbf{x}) &= g(\mathbf{x}) && \text{on } \partial\mathcal{D},\\
U(\mathbf{x}^+) &= U(\mathbf{x}^-) && \text{on } \Sigma,\\
\boldsymbol{\nu}(\mathbf{x})\cdot D(\mathbf{x}^+)\nabla U(\mathbf{x}^+) - \boldsymbol{\nu}(\mathbf{x})\cdot D(\mathbf{x}^-)\nabla U(\mathbf{x}^-)& \\
= d^C\Delta_\perp U(\mathbf{x}) && \text{on } \Sigma.
\end{aligned} \quad (19)$$

For $\mathbf{x}\in\Sigma$, we have defined $\mathbf{x}^\pm = \mathbf{x} \pm 0\boldsymbol{\nu}(\mathbf{x})$. This equation is much simpler to solve than Eqs. (9) because the jump conditions are now *local* on Σ. Notice that we have replaced $\mathbf{x}^E$ and $\mathbf{x}^I$ with $\mathbf{x}$ since the layer is sufficiently thin. Also, the diffusion equation is now posed on $\mathcal{D}\backslash\Sigma$ instead of on $\mathcal{D}\backslash\mathcal{D}^C$. The flux of photons $U(\mathbf{x})$ is continuous across the interface Σ. The current $\boldsymbol{\nu}\cdot\nabla U$ is, however, discontinuous, and its jump is given by $d^C\Delta_\perp U(\mathbf{x})$, which is also continuous since only derivatives along the interface Σ are considered.

The numerical implementation of Eqs. (19) is also relatively straightforward. Indeed let us consider the variational formulation of Eqs. (19). Upon multiplying Eqs. (19) by a test function $w(\mathbf{x})$ and integrating by parts using the Gauss formula, we obtain that

$$\begin{aligned}
&\int_{\mathcal{D}} (D(x)\nabla U(\mathbf{x})\cdot\nabla w(\mathbf{x}) + \sigma_a(\mathbf{x})U(\mathbf{x})w(\mathbf{x}))\mathrm{d}\mathbf{x}\\
&\quad + \int_\Sigma d^C\nabla_\perp U(\mathbf{x})\cdot\nabla_\perp w(\mathbf{x})\mathrm{d}S(\mathbf{x})\\
&\quad + \int_{\partial\mathcal{D}} \frac{1}{nL_n} U(\mathbf{x})w(\mathbf{x})\mathrm{d}S(\mathbf{x})\\
&\quad = \int_{\mathcal{D}} S(\mathbf{x})w(\mathbf{x})\mathrm{d}\mathbf{x} + \int_{\partial\mathcal{D}} \frac{1}{nL_n} g(\mathbf{x})w(\mathbf{x})\mathrm{d}S(\mathbf{x}).
\end{aligned} \quad (20)$$

Here $\nabla_\perp$ is the gradient operator along the surface Σ and $\mathrm{d}S$ is the surface measure on Σ and $\partial\mathcal{D}$. Since the diffusion coefficients $D(\mathbf{x})$ and $d^C(\mathbf{x})$ are positive, we obtain that the above equation is well-posed. Moreover, its discretization by the finite-element method (Galerkin projection) is straightforward, thanks to the variational formulation (20).[29] A similar variational formulation was also used to solve Eqs. (9).[22] Notice that Eqs. (19) are however, considerably simpler to solve, because the calculation and integration of the response operator $\mathcal{R}_1^C$ in Eq. (10) is replaced by a single tangential diffusion coefficient d^C.

F. Remarks on the Mathematical Model

The derivation of Eqs. (19) can be justified rigorously by using the asymptotic expansions and techniques developed in an earlier study.[23] We present the main results below and refer the reader to that study for additional details.

If we denote by ϵ the mean free path, i.e., the main distance of propagation of the photons between successive collisions, the scaling of the clear layer such that the operator KU is of order $O(1)$ is given by $L^2|\ln L| \approx \epsilon$. Discarding logarithmic terms, this means that the clear layer

must be approximately of size $\sqrt{\epsilon} \gg \epsilon$. When the clear layer is much smaller than $\sqrt{\epsilon}$, the guiding effects can be neglected as a first approximation, and classical diffusion Eqs. (4) are asymptotically valid. When the clear layer is much larger than $\sqrt{\epsilon}$, it is too large for the diffusion equilibrium $U(\mathbf{x}^E) = U(\mathbf{x}^I)$ to hold. In effect, a nonlocal equilibrium arises, which imposes that the flux of photons is asymptotically constant inside the layer. This case has been analyzed[22,23] both theoretically and numerically.

When the clear layer has the correct scaling, $L^2|\ln L| \approx \epsilon$, and the curvature of the surface Σ is uniformly positive (is a uniformly positive-definite matrix in three space dimensions), we can show[23] that the error between $u(\mathbf{x}, \mathbf{\Omega})$ and $U(\mathbf{x})$ is of order $\sqrt{\epsilon}$. The error is no longer of order ϵ as in the case of classical diffusion.[10] For typical mean free paths of order 10^{-3}–10^{-2}, the error will therefore possibly be of the order of a few percent. To further quantify this error term, in Section 4 we propose several numerical simulations.

When the clear layer is no longer scattering-free, the distance traveled by the photons when they cross the clear layer decreases, because fewer photons travel collisionless parallel to the layer boundary. This implies that the tangential diffusion coefficient also decreases. However, the final form of the generalized diffusion equation is not modified by weakly scattering layers. In the limit of strongly scattering layers, the tangential diffusion coefficient vanishes, which simply corresponds to the validity of the classical diffusion model, where the interface conditions are continuity of the flux intensity and current.

More general geometries such as oscillatory clear layers can also be considered.[13] Oscillations will also reduce the value of the tangential diffusion coefficient because photons are forced by the geometry to exit the clear layer more rapidly. Although further theoretical and numerical studies are necessary to adapt the proposed method to more complex geometries, we believe that the tangential diffusion process is a rather stable limiting process for modeling the guiding effect in clear and not-so-clear layers. All we have to do is to find an average surface Σ and then the tangential diffusion coefficient that generalizes Eqs. (14).

Let us mention finally that we restrict ourselves here to the steady-state transport equation with isotropic scattering. The generalization of the results presented below to anisotropic scattering is straightforward as long as the diffusion approximation can be justified. Time-dependent and frequency-harmonic equations also can be treated similarly as long as the variations in time of the source terms are slow compared with the characteristic mean free time, i.e., the mean time between successive collisions of the photons with the underlying medium. For time-dependent equations, the term $c^{-1}(\partial u/\partial t)$ must be added in front of Eq. (1), Eqs. (4), and the main result, Eqs. (19). In the time-harmonic case, $c^{-1} i \omega u$ is added instead, where c is the light speed and ω the modulation frequency of the source term.

4. NUMERICAL SIMULATIONS

In this section we solve Eqs. (19) numerically and compare their solution with the transport solution $u(\mathbf{x}, \mathbf{\Omega})$ obtained by a Monte Carlo algorithm. Numerical simulations are performed for both the two- and the three-dimensional problems with circular and spherical clear layers, respectively.

We assume that $S(\mathbf{x}) = 0$ and that $g(\mathbf{x}) = \delta(\mathbf{x} - \mathbf{x}_0)$, where $\mathbf{x}_0 \in \partial\mathcal{D}$ is a point on the boundary of the domain where a constant source emits light isotropically. We compare the transport and diffusion solutions by looking at the exiting currents at the boundary of the domain $\partial\mathcal{D}\backslash\{\mathbf{x}_0\}$. The transport and the diffusion currents are given by

$$J_T(\mathbf{x}) = \int_{S^{n-1}} \mathbf{\Omega} \cdot \boldsymbol{\nu}(\mathbf{x}) u(\mathbf{x}, \mathbf{\Omega}) \mathrm{d}\mu(\mathbf{\Omega}),$$

$$J_D(\mathbf{x}) = D(\mathbf{x}) \boldsymbol{\nu}(\mathbf{x}) \cdot \nabla U(\mathbf{x}), \tag{21}$$

respectively. These currents correspond to the information that is available in physical experiments.

A. Two-Dimensional Numerical Simulations

In two space dimensions, the domain $\mathcal{D}$ is the unit disk $\mathcal{D} = \{\mathbf{x} \in \mathbb{R}^2, |\mathbf{x}| < 1\}$. The surface Σ modeling the clear layer is a circle of radius R. Photons enter the domain at the point $\mathbf{x}_0 = (0, -1)$. In the numerical experiments we have chosen $R = 0.65$. The thickness of the clear layer is given by $h = 2L$; see Fig. 2. We consider several values of h. The scattering cross section $\sigma_s(\mathbf{x})$ is chosen constant and equal to 10^2 in $\mathcal{D}\backslash\mathcal{D}^C$ and vanishes in $\mathcal{D}^C$. This implies that the total size of the domain is of the order of 100 mean free paths. In all our simulations the mean free path is 0.01. We assume that there is no absorption to simplify. In the absence of a clear layer, the problem would be very much in the regime of validity of diffusion.

Transport equation (1) is solved by the Monte Carlo method.[30] Particles start at $\mathbf{x}_0$ with uniformly chosen initial direction and propagate inside the domain until they exit it. The outgoing current J_T is calculated accordingly. The number of particles 8×10^7 has been used to obtain a sufficiently small statistical variance.

Generalized diffusion model (19) is solved by Fourier decomposition after passage to polar coordinates. The jump of derivatives at the clear layer can easily be accounted for in this setting. We thus obtain a quasi-analytic expression for J_D. This is the reason that we have chosen circular clear layers.

The current at the domain boundary is discretized into 2×36 cells of size 5 deg each (or $\pi/36$). Cell 1 corresponds to the vicinity of the source, and cell 36 corresponds to the vicinity of the upper point (0, 1). The symmetry about $x = 0$ is used in the calculations. The number of particles is such that at least 15×10^3 particles exit though each cell. This ensures a statistical relative error of less than 10^{-2} by the law of large numbers, which is below or comparable to the error expected from the diffusion model for a mean free path of 10^{-2}. The lowest density is obviously obtained in the upper cell 36 and in the absence of clear layers. The corresponding diffusive flux is obtained by averaging the flux given by the Fourier expansion in each cell.

We now compare the transport and diffusion exiting currents of photons for several sizes of the clear layer.

Table 1. Relative Root-Mean-Square Error (L^2 Norm) between the Monte Carlo Simulations and the Various Diffusion Models for Several Thicknesses of the Clear Layer[a]

h	0.01	0.02	0.03	0.04	0.05	0.06	0.07
$d^C_{\text{ex-ex}}$	0.0064	0.026	0.058	0.10	0.16	0.23	0.32
$d^C_{\text{in-ex}}$	0.0029	0.0093	0.018	0.028	0.039	0.051	0.062
$d^C_{\text{in-in}}$	0.0031	0.011	0.021	0.036	0.053	0.073	0.096
d^C_{theory}	0.0124	0.0455	0.0971	0.166	0.253	0.355	0.475
$d^C_{\text{best fit}}$	0.0129	0.0465	0.0983	0.167	0.253	0.356	0.474
$E_{\text{GDM}}(\%)$	1.17	1.56	1.43	1.09	0.81	0.56	0.60
$E_{\text{BF}}(\%)$	0.73	0.65	0.57	0.49	0.46	0.47	0.46
$E_{\text{DI}}(\%)$	3.3	10.2	17.7	24.5	30.2	35.3	39.8
$E_{\text{DI2}}(\%)$	5.7	11.8	18.2	17.8	18.1	17.9	17.8

[a] The errors E_{GDM}, E_{BF}, E_{DI}, and E_{DI2} represent the relative root-mean-square error (in percent) between the Monte Carlo simulations and the generalized diffusion model obtained by using d^C_{theory}, the generalized diffusion model obtained by best fit, the classical diffusion equation, and the generalized diffusion model with tangential diffusion coefficient 1.5 times larger than d^C_{theory}, respectively.

The thickness of the clear layer varies between 1 and 7 mean free paths. According to theory, clear layers of the order of the mean free path are too small to significantly modify the solution obtained in the absence of a clear layer. Clear layers on the order of the square root of the mean free path (10 here), however, have a significant effect on the solution. Because the mean free path here is still relatively large (in the sense that its square root is not very small), we start seeing effects for clear layers of roughly 2–3 mean free paths.

Table 1 presents the results of the numerical experiments. For thicknesses h between one and seven mean free paths, the tangential diffusion coefficient defined in Eqs. (17) is given in row 4 and its three components in rows 1 to 3. The coefficient obtained by best fitting (in the least-square sense) the generalized diffusion model to the Monte Carlo data on the outgoing density between angles 60 and 180 (cells 12–36) is given in row 5. We observe that the theoretical coefficient is quite close to the best fit. This observation is confirmed by looking at the errors made by the different models. The relative L^2 norm between the Monte Carlo simulations and the various models between cells 12 and 36 is given in rows 6, 7, 8, and 9 for the generalized diffusion model, the best fit from data, the classical diffusion model with no clear layer (i.e., the diffusion coefficient is taken constant and equal to 1/200 on the whole domain), and a generalized diffusion model where the tangential diffusion coefficient has been chosen very large, respectively. By very large, we mean a tangential diffusion coefficient 1.5 times larger than its theoretical value. This solution corresponds to overestimating the guiding effect of the clear layer as we would obtain by using a diffusion approximation with a large diffusion coefficient given by Eq. (5) inside the clear layer. It is known that the correct solution is then not obtained.[13,14,22,23,28] The different models are also compared in Fig. 3 for four different thicknesses h. The graphs confirm the error estimates of Table 1.

B. Interpretation of Results

Let us first state that the generalized diffusion model deals successfully with the guiding effects caused by the presence of a clear layer. The relative root-mean-square error between transport and this diffusion model does not exceed two percent. The accuracy degrades in the vicinity of the source term (not shown), but this is typical of diffusion approximations and is independent of the clear layer. The diffusion model obtained from Eqs. (17) is almost as accurate as the best-fit model. The classical diffusion model, where the clear layer is replaced by a diffusive medium, is accurate when the clear layer is thin. However, the error becomes unacceptable in practice ($\sim$10%) even for thicknesses of the order of two mean free paths. The guiding effect is neglected, and the upward propagation of photons is clearly underestimated. The opposite effect arises when the tangential diffusion coefficient is chosen, too large. As we have already mentioned, this is similar to using the diffusion model [Eq. (5)] also inside the clear layer, which gives higher a diffusion coefficient than is physically correct and overestimates the guiding effect.

Let us conclude with a short comment on the theoretical diffusion coefficient. It is not difficult to show that asymptotically as $h \to 0$, $d^C_{\text{ex-ex}}$ is a term of order h^2, whereas the other contributions $d^C_{\text{in-ex}}$ and $d^C_{\text{in-in}}$ are terms of order $h^2|\ln h| \gg h^2$. We have observed this behavior numerically for values of h of order 10^{-4}–10^{-3}. However, in the cases shown here, where the mean free path is of order 10^{-2}, the term $d^C_{\text{ex-ex}}$, although asymptotically smaller than the other contributions, actually dominates in the calculation of the theoretical diffusion coefficient.

C. Three-Dimensional Numerical Simulations

Let us now consider the three-dimensional case. The domain is now a sphere of radius 1, the clear layer a corona of thickness h centered at $R = 0.65$, and the source is at position $(0, 0, -1)$. The transport equations are still solved by the Monte Carlo method and the diffusion equation by projection onto spherical harmonics.

We did not estimate the theoretical tangential diffusion coefficient that generalizes Eqs. (17) to the three-dimensional case. This coefficient could certainly be calculated analytically or computed numerically by assess-

ing how far photons can go on average by crossing the clear layer. However, we would rather stress another advantage that we see in Eqs. (19) as a model in optical tomography, where the photon measurements at the boundary are used to image the diffusion and absorption properties of the domain on the other side of the clear layer [i.e., close to the origin (0, 0, 0)]. We claim that the clear layer can be modeled by a possibly spatially dependent tangential diffusion coefficient provided that we have an *a priori* knowledge of its location. In other words, we claim that the inverse problem based on simulating the full clear layer (in transport, then) and the inverse problem based on replacing the clear layer by a tangential diffusion process (with *a priori* unknown strength) will give similar reconstructions, which of course come at the expense of also reconstructing the value of the tangential diffusion coefficient from the measured data. This claim corresponds to showing that the best diffusion fit yields a good approximation to the transport solution. We have seen that this is the case in two dimensions.

We now present results that confirm that this is also the case in three dimensions. The number of particles used in the calculations in 2×10^7. Such calculations are already quite long, because particles stay longer inside the domain in three dimensions than in two dimensions. Moreover, the number of particles exiting the domain in the upper part of the sphere is also smaller than in two dimensions, thus rendering our numerical simulations less accurate than in two dimensions. This situation has the advantage at least of mimicking more closely noisy measurements, and thus we regard it as an interesting benchmark. The numerical results are presented in Fig. 4. They certainly show the validity of Eqs. (19) as an accurate model to simulate the guiding effect. The root-mean-square error between the transport solution and the best-fit generalized diffusion model is of the order of 2%–3%. This error is due, moreover, mostly to random fluctuations. Other diffusion models that do not correctly account for this effect introduce too-large errors to be considered as really practical for the purpose of inver-

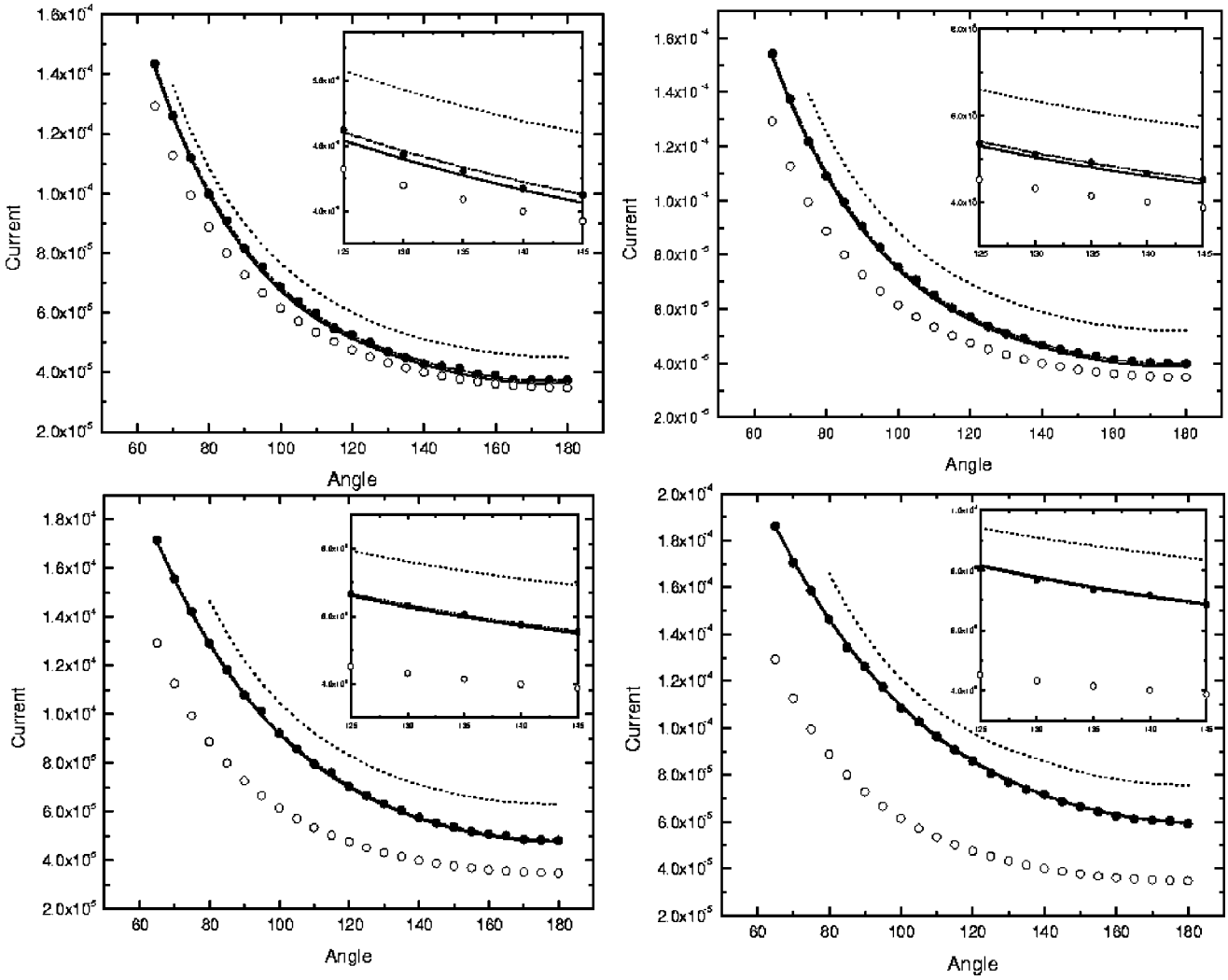

Fig. 3. Plots of the current between cells 14 (70 deg) and 36 (180 deg) at the boundary of the unit disk (two-dimensional simulation) for the Monte Carlo solution and the different diffusion models. The thickness of the clear layer in mean free path is 2, 3, 5, and 7 for the top-left, top-right, bottom-left, and bottom-right figures, respectively. Solid circles, Monte Carlo simulation; open circles, classical diffusion model; solid curves, generalized diffusion model with theoretical tangential diffusion coefficient; dashed–dotted curves, generalized diffusion model with best fit; dotted curves, generalized model with large tangential diffusion coefficient. The inset represents a magnification of the above results between angles 125 and 145.

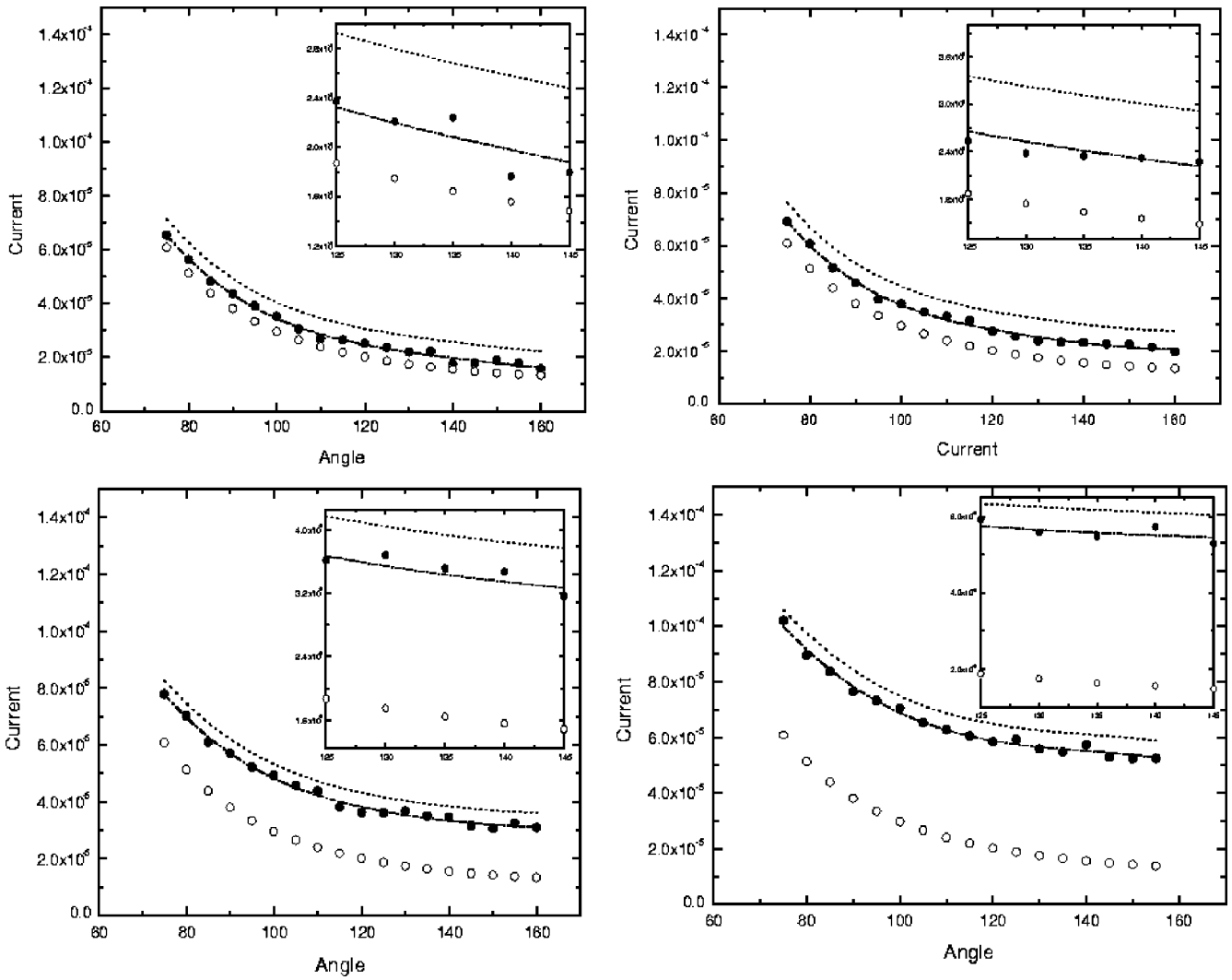

Fig. 4. Plots of the current between cells 15 (75 deg) and 32 (160 deg) at the boundary of the unit sphere (three-dimensional simulation with azimuthal symmetry) for the Monte Carlo solution and the different diffusion models. The thickness of the clear layer in mean free path is 1, 2, 4, and 6 for the top-left, top-right, bottom-left, and bottom-right figures, respectively. Solid circles, Monte Carlo simulation; open circles, classical diffusion model; solid curves, generalized diffusion model with theoretical tangential diffusion coefficient; dashed–dotted curves, generalized diffusion model; dotted curves, generalized model with large tangential diffusion coefficient. The inset represents a magnification of the above results between angles 125 and 145.

sion of physical properties from boundary measurements.[13,14,22,23,28] For instance, the classical diffusion model in our simulations produces results as far as 50% off the transport solution.

5. CONCLUSIONS

We propose a generalized diffusion model that accounts for the multiple scattering of photons in highly scattering media (classical diffusion regime) as well as for the near-collisionless propagation of the same photons in clear layers (purely transport regime resulting in a guiding effect).

This model can be derived mathematically from the phase-space radiative transport equation as a small mean-free-path limit. It captures the guiding effect of photons in the clear layer quite well. Moreover, it has almost the same cost as the classical diffusion model, which fails completely to model the clear-layer effects, and a lower cost than previously derived generalized diffusion equations, which are already much less expensive than full transport solutions. The reason for this lower cost is that the nonlocal interface conditions of the previously derived diffusion models are replaced by the models' best local approximations. The best local approximation takes the form of a tangential diffusion process.

The strength of the tangential diffusion process can be calculated analytically or numerically provided that one has access to the geometry of the clear layer. We have shown numerically that when this geometry is unknown or only partially known, the diffusion process that best fits the effect of the clear layer gives boundary measurements that are visually indistinguishable from the measurements obtained by solving the full transport equations. We believe that the generalized diffusion model can thus be used safely in optical tomography as an accurate approximation of the forward model.

It remains to apply the method to the inverse problem,[14] which consists of reconstructing $\sigma_a(\mathbf{x})$ and

$D(\mathbf{x})$ from boundary measurements. The validation of the method to solve the inverse problem with more general geometries for the clear layer, both for the steady-state equations and for the time-domain or frequency-domain[1] equations, is the subject of ongoing research.

ACKNOWLEDGMENTS

The authors thank the reviewers for their constructive comments. This research was supported in part by National Science Foundation grant DMS-0233549 and by U.S. Office of Naval Research grant N00014-02-1-0089.

REFERENCES

1. S. R. Arridge, "Optical tomography in medical imaging," Inverse Probl. **15**, R41–R93 (1999).
2. A. Y. Bluestone, G. S. Abdoulaev, C. Schmitz, R. L. Barbour, and A. H. Hielscher, "Three-dimensional optical-tomography of hemodynamics in the human head," Opt. Express **9**, 272–286 (2001), optics-express.org.
3. O. Dorn, "A transport-backtransport method for optical tomography," Inverse Probl. **14**, 1107–1130 (1998).
4. V. A. Markel and J. C. Schotland, "Inverse problem in optical diffusion tomography. I. Fourier–Laplace inverse formula," J. Opt. Soc. Am. A **18**, 1336–1347 (2001).
5. V. A. Markel and J. C. Schotland, "Inverse problem in optical diffusion tomography. II. Role of boundary conditions," J. Opt. Soc. Am. A **19**, 558–566 (2002).
6. G. J. Müller, ed., *Medical Optical Tomography: Functional Imaging and Optical Technologies*, IS Series Vol. IS11 (SPIE Press, Bellingham, Wash., 1993).
7. F. Natterer and F. Wübbeling, *Mathematical Methods in Image Reconstruction*, SIAM Monographs on Mathematical Modelling and Computation (SIAM, Philadelphia, Pa., 2001).
8. "Session on Optical Tomography and Optical Imaging," Progress in Electromagnetic Research Symposium (PIERS), July 1–5, 2002, Cambridge, Massachusetts.
9. A. D. Klose and A. H. Hielscher, "Optical tomography using the time independent equation of radiative transfer," J. Quant. Spectrosc. Radiat. Transf. **72**, 715–732 (2002).
10. R. Dautray and J.-L. Lions, *Mathematical Analysis and Numerical Methods for Science and Engineering* (Springer-Verlag, Berlin, 1993), Vol. 6.
11. E. W. Larsen and J. B. Keller, "Asymptotic solution of neutron transport problems for small mean free paths," J. Math. Phys. **15**, 75–81 (1974).
12. A. H. Hielscher, R. E. Alcouffe, and R. L. Barbour, "Comparison of finite-difference transport and diffusion calculations for photon migration in homogeneous and heterogeneous tissues," Phys. Med. Biol. **43**, 1285–1302 (1998).
13. J. Ripoll, M. Nieto-Vesperinas, S. R. Arridge, and H. Dehghani, "Boundary conditions for light propagation in diffuse media with non-scattering regions," J. Opt. Soc. Am. A **17**, 1671–1681 (2000).
14. H. Dehghani, S. R. Arridge, M. Schweiger, and D. T. Deply, "Optical tomography in the presence of void regions," J. Opt. Soc. Am. A **17**, 1659–1670 (2000).
15. S. R. Arridge and J. C. Hebden, "Optical imaging in medicine: II. Modelling and reconstruction," Phys. Med. Biol. **42**, 841–853 (1997).
16. C. K. Hayakawa, J. Spanier, F. Bevilacqua, A. K. Dunn, J. S. You, B. J. Tromberg, and V. Venugopalan, "Perturbation Monte Carlo methods to solve inverse photon migration problems in heterogeneous tissues," Opt. Lett. **26**, 1335–1337 (2001).
17. G. Bal and Y. Maday, "Coupling of transport and diffusion models in linear transport theory," M2AN Math. Model. Numer. Anal. **36**, 69–86 (2002).
18. G. Bal and X. Warin, "Discrete ordinate methods in xy-geometry with spatially varying angular discretization," Nucl. Sci. Eng. **127**, 169–181 (1997).
19. F. Golse, S. Jin, and C. D. Levermore, "The convergence of numerical transfer schemes in diffusive regimes. I. Discrete-ordinate method," SIAM (Soc. Ind. Appl. Math.) J. Numer. Anal. **36**, 1333–1369 (1999).
20. E. W. Larsen, J. E. Morel, and W. F. Miller, Jr., "Asymptotic solutions of numerical transport problems in optically thick, diffusive regimes," J. Chem. Phys. **69**, 283–324 (1987).
21. M. Tidriri, "Asymptotic analysis of a coupled system of kinetic equations," C. R. Acad. Sci. Paris Ser. I Math. **t.328**, 637–642 (1999).
22. G. Bal, "Particle transport through scattering regions with clear layers and inclusions," J. Comput. Phys. **180**, 659–685 (2002).
23. G. Bal, "Transport through diffusive and non-diffusive regions, embedded objects, and clear layers," SIAM (Soc. Ind. Appl. Math.) J. Appl. Math. **62**, 1677–1697 (2002).
24. M. Choulli and P. Stefanov, "Reconstruction of the coefficients of the stationary transport equation from boundary measurements," Inverse Probl. **12**, L19–L23 (1996).
25. A. Tamasan, "An inverse boundary value problem in two-dimensional transport," Inverse Probl. **18**, 209–219 (2002).
26. G. Bal, V. Freilikher, G. Papanicolaou, and L. Ryzhik, "Wave transport along surfaces with random impedance," Phys. Rev. B **62**, 6228–6240 (2000).
27. J. M. Luck and T. M. Nieuwenhuizen, "Light scattering from mesoscopic objects in diffusive media," Eur. Phys. J. B **7**, 483–500 (1999).
28. M. Firbank, S. A. Arridge, M. Schweiger, and D. T. Delpy, "An investigation of light transport through scattering bodies with non-scattering regions," Phys. Med. Biol. **41**, 767–783 (1996).
29. S. C. Brenner and L. R. Scott, *The Mathematical Theory of Finite Element Methods* (Springer-Verlag, New York, 2002).
30. J. Spanier and E. M. Gelbard, *Monte Carlo Principles and Neutron Transport Problems* (Addison-Wesley, Reading, Mass., 1969).